Adequacy of Lumped Parameter Models for SCR Reactors with Monolith Structure

Enrico Tronconi and Pio Forzatti
Dipartimento di Chimica Industriale e Ingegneria Chimica "G. Natta" del Politecnico, I-20133 Milano, Italy

Two- and one-dimensional steady-state isothermal mathematical models of monolith reactors for selective catalytic reduction (SCR) of NO_x by NH_3 are compared for circular, square and triangular geometry, as well as for linear and Rideal kinetics. Solutions for the two-dimensional model demonstrate that, as the reaction rate decreases from infinity to zero, the Sherwood number varies from the values of the Nusselt number characteristic of the Graetz-Nusselt problem with constant wall temperature to those with constant wall heat flux but with peripherally varying temperature. A lumped-parameter treatment, based on similarity with the constant wall temperature heat transfer problem, agrees satisfactorily with the solutions for a far more expensive two-dimensional model. The agreement is excellent for square channels, but the NH_3 slip tends to be underestimated in the triangular geometry. The one-dimensional model reproduces successfully experimental effects of the NH_3/NO feed ratio, and of the area velocity and the size of monolith channels.

Introduction

Emissions of nitrogen oxides (NO_x) from power plant flue gases pose a paramount environmental problem, causing photochemical smog and acid rains. To control NO_x emissions, techniques have been developed that modify the combustion process to reduce the formation of nitrogen oxides or treat effluents to remove NO_x. Among flue gas treatment methods, the SCR (selective catalytic reduction) process, which converts NO_x to nitrogen and water by using ammonia as a reducing agent, has gained significant industrial applications. The process offers high NO_x removal efficiency and selectivity (Bosch and Janssen, 1988).

Many SCR plants are now operated in Japan, Germany, and Austria, and the technology is being considered for extensive applications in other European countries as well as in the U.S. Commercial catalysts are Ti-W-V oxides (Bosch and Janssen, 1988) or zeolite-based systems (Kiovsky et al., 1980), employed as monolithic materials with a honeycomb structure or in a plate-type form (Bosch and Janssen, 1988; Boer et al., 1990). The unique advantages of such catalyst structures are very low pressure drops and high geometric surface areas per unit volume. However, the flow in monolith channels is usually laminar, resulting in slow interphase transport. Considerable work has been done on modeling and analyzing general monolith (or catalytic wall) reactors (Carberry and Kulkarni, 1973; Votruba et al., 1975a; Smith and Carberry, 1975; Hlavacek and Votruba, 1976; Heck et al., 1974; Hegedus, 1975; Young and Finlayson, 1976a, b; Pereira et al., 1988). Since this class of reactors has been applied mostly to automotive catalytic converters (Taylor, 1984) and to catalytic combustors (Trimm, 1980; Pfefferle and Pfefferle, 1988), emphasis has been placed primarily on the analysis of strong thermal effects, multiplicity of steady states, and other phenomena associated with very fast exothermic reaction conditions, that is, in a purely diffusional regime.

On the other hand, virtually isothermal conditions prevail in SCR reactors because of the very low concentrations of the reactants. In addition, under power plant conditions, the SCR reaction is approximately as fast as external diffusion.

Analyses of the monolith reactor addressing the issues specific to SCR applications are scarce in the scientific literature. Binder-Begsteiger et al. (1990) have presented a simplified analytical treatment of the SCR reactor valid only for a purely diffusion-controlled operation. Taking advantage of isothermality, Buzanowski and Yang (1990) have recently derived a simple one-dimensional analytic solution for the SCR monolith

Correspondence concerning this article should be addressed to P. Forzatti.

reactor, which yields NO conversion as an explicit function of the space velocity. Their solution, however, applies only to kinetics exhibiting first order with respect to NO and zero order with respect to NH_3, which is not appropriate for industrial SCR plants operating with substoichiometric NH_3/NO ratios where kinetic dependence on NH_3 is apparent. Furthermore, the authors dismiss the influence of interphase transport resistances and do not mention how to estimate the gas-solid mass transfer coefficient of their equations. This conclusion probably is attributed to the very small size of the monolith channels used in their investigation as compared to standard SCR monoliths.

Shortly before submission of this article, Beekman and Hegedus (1991) published work on a comprehensive one-dimensional model of the monolith SCR reactor, which includes Langmuir-Hinshelwood kinetics and full accounts of both intra- and inter-phase diffusional phenomena. Model predictions reported compare successfully with the data. The authors present an interesting industrial application to optimization of the morphological properties of the catalyst, but do not address the adequacy of a lumped parameter treatment of the SCR monolith reactor, which is the focus of this article. Indeed, they evaluate local mass transfer coefficients for NO and NH_3 according to Hawthorn's equation (Hawthorn, 1974), which was actually developed for prediction of length-mean coefficients in a purely diffusional regime.

Much more basic and simplified approaches can be found in the technical literature on SCR processes. All of the above mentioned treatments for design and analysis of SCR reactors rely on lumped parameter (one-dimensional) models accounting only for the axial concentration gradients inside the catalyst channels and are computationally much simpler than two-dimensional approaches, where radial gradients also are considered. The one-dimensional model actually lumps the complexities of the radial interphase transport into a gas-solid mass transfer coefficient (or a Sherwood number in dimensionless form). For its evaluation, a customary approximation invokes a complete analogy with the Graetz-Nusselt problem governing heat transfer to a fluid in laminar flow in a duct with constant wall temperature (Hawthorn, 1974). In this approach, the Sherwood number is taken to equal the Nusselt number for the same duct shape, which is generally available (for example, Shah and London, 1978). This is an approximate procedure, since the boundary condition at the wall of the monolith reactor does not match the assumption of constant wall temperature in the heat transfer problem.

Brauer and Schlüter (1965) showed that a finite rate of reaction at the wall of a catalytic wall tubular reactor can influence significantly the values of the Sherwood number. Relevant results in this respect are contained in a pioneering work by Heck et al. (1976), who compared one- and two-dimensional models of nonisothermal cylindrical monolith reactors for automobile catalytic converters. They found that the two models would yield very similar results provided that appropriate boundary conditions of the Graetz-Nusselt problem were used when invoking the analogy between heat and mass transfer. The nonisothermal conditions involved in this work, however, prevented a rationalization of the relationship between interphase transport coefficients and reaction kinetics. Also, the influence of the monolith geometry was not explored in this respect.

In the following, we first derive a steady-state, isothermal, two-dimensional model for diffusion and reaction in a monolith honeycomb catalyst. For first-order kinetics and for three-channel geometries (circular, square, and equilateral triangular), the model equations are solved to study the effect of the rate of reaction at the catalytic wall on the dimensionless mass transfer coefficient (Sherwood number). Then, the two-dimensional simulation is compared with a simple one-dimensional model which relies on the analogy between mass and heat transfer to assess the adequacy of lumped parameter models for SCR reactors. We also extend the analysis to include more appropriate Rideal kinetics for the SCR reaction, and to evaluate the entrance effects associated with a developing laminar velocity profile. Predictions of NO conversion generated by the resulting treatment are finally compared with existing data measured in laboratory monolith reactors.

Since the emphasis of this work is on gas-solid mass transport, we will assume that the reaction takes place on the monolith wall, and consider global rate constants by incorporating the influence of intraporous diffusional resistances. In a forthcoming article, the present model will be extended to include the effects of the catalyst pore structure, thus allowing prediction of the monolith catalyst behavior from its intrinsic kinetics and eventually comparison of catalyst performances.

Results and Discussion

Two-Dimensional Analysis of the Monolith Reactor

We consider an SCR monolith catalyst with honeycomb matrix, and assume: a) identical conditions within each channel; b) constant fluid properties; c) isothermal conditions; d) fully developed laminar velocity profile in the channels; e) negligible axial diffusion; and f) irreversible first-order kinetics at the catalytic wall. Assumption a implies that simulation of a single monolith channel is sufficient to represent the behavior of the whole reactor: it may be invalid in the huge industrial SCR reactors due to imperfect distribution of NH_3 in the feed as well as to unequal velocity and temperature distributions. Assumptions b and c are quite reasonable for SCR conditions (Buzanowsky and Yang, 1990). Assumption d will be discussed further in a following section. Axial molecular diffusion effects are important only at low values of $Pe = (u_m D_h/D_{NO})$ (Gill and Suwandi, 1967). Finally, linear kinetics in NO are applicable to the SCR reaction if it occurs in the presence of an excess of NH_3 (Inomata et al., 1980; Wong and Nobe, 1986; Bosch and Janssen, 1988; Buzanowsky and Yang, 1990).

We then define the following dimensionless variables and parameters:

- Reduced NO gas-phase concentration: $\Gamma = C_{NO}/C^{\circ}_{NO}$
- Dimensionless axial distance: $z^* = (z\ D_{NO})/(u_m\ D_h^2) = (z/D_h)/(Re\ Sc)$
- Dimensionless velocity profile: $\varphi = u(x,y)/u_m$
- Damkohler number: $Da = k_C\ D_h/D_{NO}$

Note that the hydraulic diameter D_h is taken as the characteristic size of the channel geometry.

The equation governing steady-state diffusion and reaction of NO in each monolith channel can be written in dimensionless form as:

$$\varphi \frac{\partial \Gamma}{\partial z^*} = \nabla^2 \Gamma \tag{1}$$

$$\nabla^2 = \frac{\partial^2}{\partial r^{*2}} + \frac{1}{r^*}\frac{\partial}{\partial r^*} \quad \text{for the circular channel (cylindrical coordinates)}$$

$$\nabla^2 = \frac{\partial^2}{\partial x^{*2}} + \frac{\partial^2}{\partial y^{*2}} \quad \text{for the square and triangular channel (Cartesian coordinates)}$$

with initial condition:

$$\Gamma = 1 \text{ at } z^* = 0 \quad \text{at the channel inlet,} \tag{2}$$

and boundary conditions:

$$\text{symmetry} \qquad \text{at the channel axis} \tag{3}$$

$$-\frac{\partial \Gamma}{\partial n^*} = -Da\,\Gamma \quad \text{at the catalytic wall} \tag{4}$$

where n represents the outward direction normal to the wall.

The cup-mixing average concentration of NO over the channel cross-section S is:

$$\Gamma_m = \frac{\int_S \varphi\,\Gamma\,dS}{\int_S \varphi\,dS} \tag{5}$$

A local Sherwood number is defined as:

$$\mathrm{Sh} = \frac{-\left.\frac{\partial \Gamma}{\partial n^*}\right|_P}{\Gamma_m - \Gamma_p} = \frac{Da\,\Gamma_P}{\Gamma_m - \Gamma_P} \tag{6}$$

In Eq. 6, the subscript P indicates a peripheral average on the boundary, that is, on the contour of the monolith channel cross-section.

On the formal basis, the SCR reactor problem represented by Eqs. 1-6 appears quite similar to the Graetz-Nusselt problem (Shah and London, 1978; Grigull and Tratz, 1965), but for the boundary condition at the wall, Eq. 4. Such a condition introduces the effect of a finite rate of reaction at the wall as compared to the rate of diffusional transport. The importance of the chemical process (catalytic reaction at the wall) relative to that of the physical process (diffusional transport of NO) is governed by the Damkohler number Da. Dimensional analysis specifies that the reduced NO concentration Γ and the Sherwood number are functions both of the reduced axial coordinate z^* and of Da. This implies a remarkable difference with the Graetz-Nusselt problem, where the dimensionless temperature and the local dimensionless heat transfer coefficient (Nusselt number) are uniquely functions of the relevant reduced axial coordinate, since no chemical phenomenon interferes with the diffusional transport of heat in this case.

An exact analogy between the SCR reactor problem and the Graetz-Nusselt problem with constant wall temperature, however, is recovered in the limit of infinitely fast kinetics ($Da \to \infty$), which corresponds to a purely physical regime with $\Gamma \to 0$ at the wall. Thus, it is expected that values of the Sherwood number calculated from Eqs. 1-6 should converge to the solutions of the Graetz-Nusselt problem with constant wall temperature for large Damkohler numbers, as confirmed, for example, by calculations of Brauer and Schlüter (1965) and Bräuer and Fetting (1966) for tubular catalytic wall reactors.

A second asymptotic case is procured in the limit of infinitely slow kinetics ($Da \to 0$), which implies a purely chemical regime. Bräuer and Fetting (1966) showed that in tubular catalytic wall reactors, the local Sherwood numbers at low values of Da tend to match the Nusselt numbers from the solution of the Graetz-Nusselt problem with constant heat flux at the wall.

For typical SCR power plant conditions, however, Da is of the order unity. Then, neither one of the two asymptotic cases above appears adequate in principle for estimation of the mass transfer coefficients in SCR reactors. The extent of variation of the Sherwood number with the rate of reaction is investigated on a quantitative basis in the following section for circular monolith channels, as well as for square and triangular (equilateral) ducts, which are more representative of the actual shape of SCR monolith reactors in the case of honeycomb and of a class of plate-type catalysts, respectively.

Sherwood numbers from model solutions

Equations 1-6 have been solved numerically for a circular, square and equilateral triangular duct. For each geometry, the exact expression of the laminar, fully developed velocity profile $\varphi(r^*)$ or $\varphi(x^*, y^*)$ has been used as given by Shah and London (1978).

Orthogonal collocation techniques (Villadsen and Stewart, 1967; Villadsen and Michelsen, 1978; Finlayson, 1980) were applied to the radial discretization of the concentration profiles in one dimension (circle) and two dimensions (square and triangle), while the library routine LSODI was employed for integration of the resulting set of ODEs along z^*. In the case of the equilateral triangular duct, the transformation of the coordinate system for irregular domains described by Young (1974) and Young and Finlayson (1976a, b) has been exploited. The adequacy of the numerical algorithms was tested by solving the Graetz-Nusselt problem with constant wall temperature in each geometry and by comparing the calculated asymptotic Nusselt numbers with those listed in Shah and London (1978) and in Young and Finlayson (1976a).

For the three duct geometries considered, Figure 1 shows the effect of the reaction kinetics (Da) on the local Sherwood numbers, calculated according to Eq. 6 and plotted against the dimensionless axial coordinate z^*. In all cases, Sherwood numbers decrease rapidly along the entry region of the channel until an asymptotic value (Sh_∞) is reached. Such a value depends on the geometry as well as on Da. The combined effects of the kinetics and of the duct geometry on Sh_∞ are summarized in Figure 2.

The influence of the geometry on Sh is found in line with that on the conversion. For the same Da, the circular duct always yields the highest Sherwood numbers as well as the highest conversion, and the triangular duct yields the smallest with the square duct in-between. In fact, the fluid mean effective diffusion path length is greater for ducts with acute corners, resulting in lower reactant concentrations at the corners relative to other wall locations away from the corners.

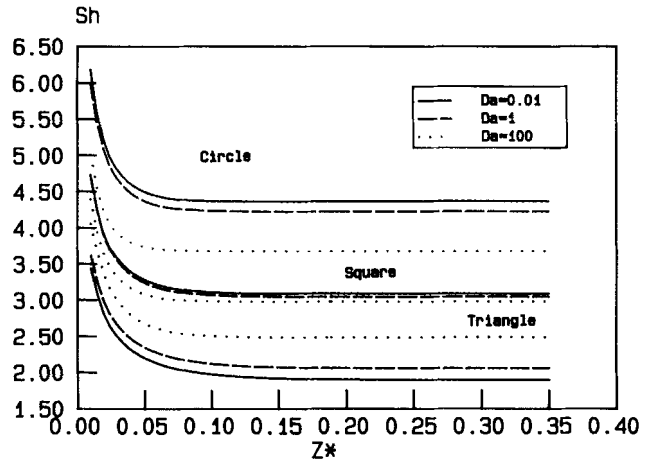

Figure 1. Local Sherwood number *Sh* as a function of the dimensionless axial coordinate of the monolith reactor z^* and of the Damkohler number *Da* for the circular, square and equilateral triangular geometry of the monolith channel cross-section.

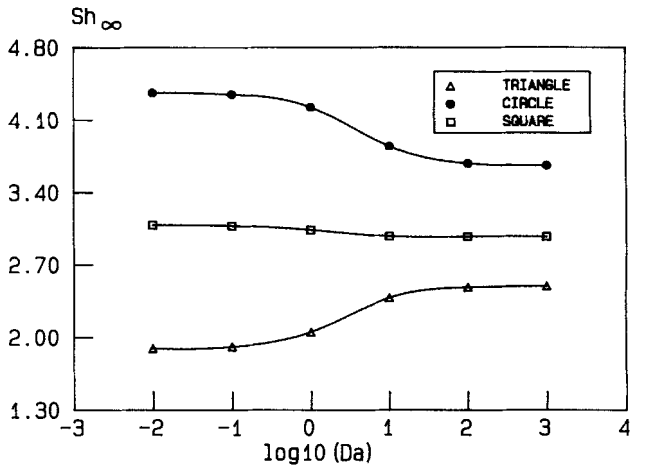

Figure 2. Influence of the Damkohler number *Da* and the channel geometry on the asymptotic Sherwood number Sh_∞.

Thus, the peripheral average wall concentration Γ_P is lower too. According to Eq. 6, for the same Damkohler number this results in smaller values of *Sh*. For the same reason, the overall conversion is reduced. Table 1 shows the differences in Γ_P among the three geometries for $Da = 1$.

Concerning the influence of the Damkohler number on *Sh*, the two-dimensional analysis of the monolith reactor reveals that a finite rate of reaction considerably affects the values of the mass transfer coefficients. The effect of *Da* on *Sh*, however, is different both in extent and in trend for the three geometries. As shown in Figure 2, for the circular duct increasing the Damkohler number, that is, going toward faster kinetics, reduces the asymptotic Sherwood number. In the case of the square duct, we note a much smaller reduction of *Sh*. For the triangular duct, on the contrary, *Sh* increases with increasing *Da*. Thus, when the kinetics are slow, asymptotic mass transfer coefficients calculated by the analogy with the Graetz problem with constant wall temperature may be underestimated by as much as 20% for circular channels, but overestimated up to 25% in the case of equilateral triangular ducts.

Such peculiar dependences can be interpreted by noting first that for each geometry, the limiting values of Sh_∞ for $Da \to \infty$ and for $Da \to 0$ correspond to the asymptotic Nusselt numbers for constant wall temperature ($Nu_{\infty,T}$) and for constant heat flux ($Nu_{\infty,H}$), respectively, as shown in Table 2. Thus, the dependence of *Sh* and *Da* can be rationalized by analogy with the influence of the boundary conditions on *Nu* in the Graetz problem, where it is well known that a steeper wall temperature gradient is observed for the constant-flux than for the constant-temperature boundary condition (Shah and London, 1978). In the latter case, an inflection point arises in the radial temperature profile, which results in a smaller gradient at the wall.

Due to the analogy with the Graetz problem, we expect that decreasing *Da* increments the wall concentration gradient in monoliths of any geometry. For circular channels, this results directly in an enhanced Sherwood number, according to Eq. 6. For noncircular, cornered ducts however, reducing *Da* brings about peripheral nonuniformities of the wall concentration, which adversely affect *Sh*, as already discussed.

Thus, the overall impact of *Da* on *Sh* is determined by a balance between two competing effects. They almost compensate each other in the case of the square duct: noticeably, for the square geometry, which is most common in ceramic mon-

Table 1. Effect of Channel Geometry on the Peripheral Average of NO concentration at the catalyst wall, Γ_P*

Geometry	Γ_P/Γ_m
Circle	0.809
Square	0.753
Equilateral Triangle	0.672

*Calculated asymptotic values of the ratio Γ_P/Γ_m for the circular, square and equilateral triangular geometry. $Da = 1$, $z^* > 0.2$.

Table 2. Asymptotic Sherwood vs. Nusselt Numbers for Various Geometries

	(This Work)		(Shah and London, 1978)	
Geometry	Sh_∞, $Da = 0.01$	Sh_∞, $Da = 1{,}000$	$Nu_{\infty,H}$*	$Nu_{\infty,T}$
Circle	4.362	3.659	4.364	3.657
Square	3.087	2.977	3.091	2.976
Equilateral Triangle	1.891	2.494	1.89	2.47 (2.491)**

*Values of $Nu_{\infty,H}$ correspond to solutions of the Graetz-Nusselt problem with boundary condition H2 in Shah and London (1978): that is, constant axial wall heat flux with uniform peripheral wall heat flux, but with peripherally varying temperature.
**Young and Finlayson (1976a).

olith catalyst for $DeNO_x$ applications, the mass transfer coefficients appear to be nearly insensitive to the reaction kinetics, as shown in Figure 2. However, the adverse influence of the geometry prevails in the acute cornered triangular duct, causing Sh to decrease with decreasing Da, a reversal of the trend noted for the circular duct.

Along similar lines, in the case of monoliths with other channel geometries the range of variation of Sh with Da can be evaluated *a priori* by examining the limiting Nusselt numbers $Nu_{\infty,H}$ and $Nu_{\infty,T}$ for the same duct geometry. It is worth emphasizing that $Nu_{\infty,H}$ corresponds to solutions of the Graetz-Nusselt problem with constant axial wall heat flux and with uniform peripheral wall heat flux, but with peripherally varying wall temperature: this is the thermal boundary condition $H2$ according to Shah and London (1978).

Notably, mass transfer coefficients in monoliths have been determined experimentally in the absence of chemical reaction, for example, by evaporation experiments (Votruba et al., 1975). Such measurements yield estimates corresponding to a purely diffusional regime ($Da \rightarrow \infty$). Therefore, when a finite rate of reaction prevails in the monoliths, these estimates are expected to differ from the actual mass transfer coefficients to the extent shown in Figures 1 and 2.

Lumped parameter model of the monolith reactor

In the following one-dimensional treatment, we introduce the same assumptions of the two-dimensional model, but we consider only average values for velocity (u_m) and concentration (Γ_m) over the channel cross-section in the gas phase and a peripheral average of the concentration over the catalytic wall (Γ_P).

A steady-state mass balance of the single reactant in the gas phase yields in this case:

$$\frac{d\Gamma_m}{dz^*} = -4\, Sh(z^*)\,(\Gamma_m - \Gamma_P) \tag{7}$$

with $\Gamma_m = 1$ at $z^* = 0$.

For the same reactant, a mass balance at the wall gives:

$$Sh\,(\Gamma_m - \Gamma_P) = Da\,\Gamma_P \tag{8}$$

If Eq. 8 is used to eliminate Γ_P, Eq. 7 becomes:

$$\frac{d\Gamma_m}{dz^*} = -4\,\frac{Da\,Sh}{Da + Sh}\,\Gamma_m \tag{9}$$

Integration of Eq. 9 yields axial profiles of the average gas concentration Γ_m, which can be compared with similar profiles calculated by the two-dimensional model.

The goodness of this simplified model depends on the adequacy of the expression used to evaluate Sh. If values of the local Sherwood number $Sh(z^*, Da)$ taken from solutions of the distributed parameter model (Figure 1) were used in integrating Eq. 9, then the lumped-parameter model would match the two-dimensional treatment identically.

In the following, we adopt an alternative approximation, which is essentially the approach proposed in the technical literature on monolith reactors: $Sh(z^*, Da)$ is assumed to be equal to $Nu_T(z^*)$, the Nusselt number from solution of the

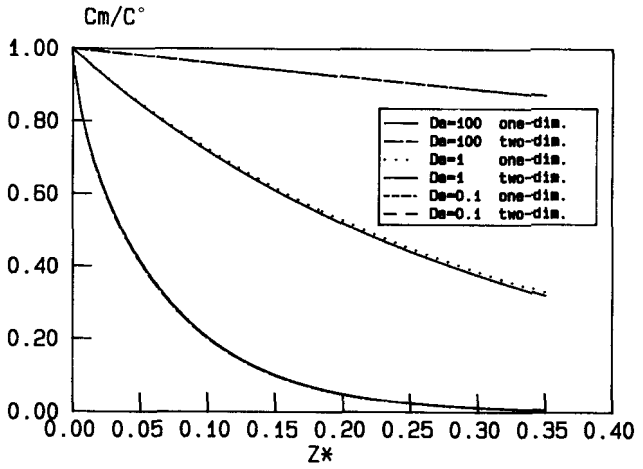

Figure 3. One-Dimensional vs. two-dimensional monolith reactor models.

Calculated axial profiles of the average reactant concentration Γ_m for various Damkohler numbers; first-order kinetics; case of circular channels.

Graetz problem for constant wall temperature. As discussed previously, this amounts to neglecting the influence of the kinetics on the dimensionless mass transfer coefficient.

The expression used for Sh is then given by:

$$Sh = Nu_{\infty,T} + 6.874\,(1{,}000\,z^*)^{-0.488}\,\exp(-57.2\,z^*) \tag{10}$$

Equation 10 is adapted from the solution of the Graetz problem in circular ducts for constant wall temperature originally proposed by Grigull and Tratz (1965). For each duct geometry, the values of $Nu_{\infty,T}$ are listed in the fourth column of Table 2.

Lumped vs. distributed parameter model

To rate the adequacy of the approximation involved in Eq. 10, conversion profiles resulting from solutions of Eqs. 9 and 10 have been compared with exact two-dimensional solutions

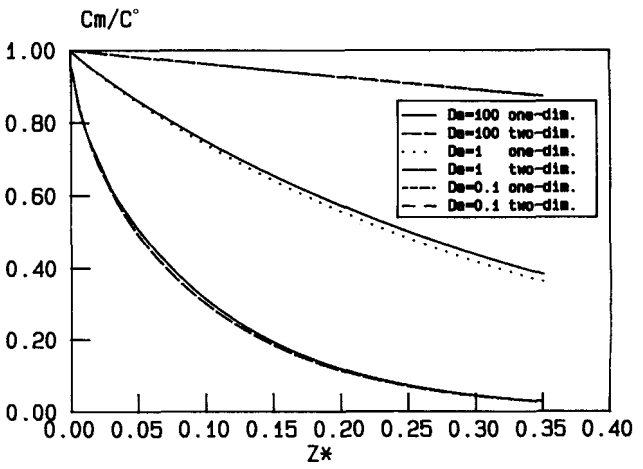

Figure 4. One-dimensional vs. two-dimensional monolith reactor models.

Calculated axial profiles of the average reactant concentration Γ_m for various Damkohler numbers; first-order kinetics; case of equilateral triangular channels.

for different reaction kinetics (Da) and for the three duct geometries. Results are shown in Figures 3-4 for the circular and triangular geometry.

The differences between one-dimensional and two-dimensional model solutions are minor in all cases. For each geometry, the exact conversion profile for $Da = 100$ is almost indistinguishable from the approximate one, confirming that Eq. 10 is accurate in the limit of very fast kinetics. The minor differences apparent in the case of the triangular cross-section (Figure 4) are due to the fact that Eq. 10 reproduces only approximately the dependence $Sh(z^*)$ for geometries other than the circle.

Some limited deviations become apparent in Figures 3-4 in the intermediate case of $Da = 1$: here, the lumped parameter model slightly underestimates the conversion for the circular duct, is practically correct for the square duct, and slightly overpredicts the conversion in the triangular channel. Such a behavior is completely in line with the dependence of the Sherwood number on the reaction kinetics demonstrated in Figure 2, which is properly accounted for in the two-dimensional model but is neglected in the lumped model.

Finally, in the case of slow kinetics ($Da = 0.1$), the two models again yield very similar predictions, as expected. The reactor performances are controlled here by kinetics rather than by mass transfer, so that approximations in the estimates of Sh do not affect the calculated conversion significantly.

Thus, the results in Figures 3-4 legitimize quantitatively the use of the approximate lumped parameter model as long as first-order kinetics are applicable. The suitability of the one-dimensional treatment for Rideal kinetics will be addressed in the next section. It is worth mentioning, however, that the interaction between kinetics at the catalytic wall and interphase transport processes is expected to play a much more significant role in the case of nonisothermal conditions, such as those prevailing in monolithic catalytic combustors or catalytic mufflers. Here, strong thermal effects make the reactor behavior remarkably more sensitive to modifications in the interphase transport of heat and mass. Analysis of these conditions, which are not typical of SCR reactors, is beyond the scope of this work. Nevertheless, it may be relevant to recall a result reported by Heck et al. (1976), who compared one- and two-dimensional models of cylindrical monolithic reactors for automobile catalytic converters. These authors found that a satisfactory match between the two models was achieved when the gas-solid transport coefficients were evaluated from the Graetz solutions for constant wall flux prior to the light-off (ignition) of the combustion reaction (in the region of flow kinetics) and from the solutions for constant wall temperature thereafter (in the region of fast kinetics). Such results are readily interpreted in the light of the influence of the reaction kinetics on transport coefficients discussed in the previous section.

Case of Rideal Kinetics

In the previous analyses, first-order kinetics were always assumed. The rate of the SCR reaction is actually first order with respect to NO and essentially zero order with respect to NH_3 (Inomata et al., 1980; Bosch and Janssen, 1988; Buzanowski and Yang, 1990) as long as NO is the limiting reactant [α = feed ratio (NH_3 / NO) > 1]. This is not the case, however, in typical SCR applications for power plants, where a substoichiometric feed ratio ($\alpha < 1$) is employed to minimize the "slip" of unconverted ammonia. When NH_3 becomes the limiting reactant, a kinetic dependence on ammonia is also apparent (Binder-Begsteiger et al., 1990).

A rate expression in agreement with these observations is given by:

$$-dc_{NO}/dt = k_c\, C_{NO}\, \Theta_{NH3} = \frac{k_c\, C_{NO}\, K_{NH3}\, C_{NH3}}{1 + K_{NH3}\, C_{NH3}} \qquad (11)$$

where Θ_{NH3} represents the fractional surface coverage of ammonia adsorbed on the catalyst-active sites. If the influence of O_2 is neglected, Eq. 11 can be derived assuming a Rideal mechanism where NO in the gas phase reacts with NH_3 strongly adsorbed on the catalyst. Experimental evidence in favor of such a mechanism on SCR $V_2O_5 - TiO_2$ catalysts is available (Rajadhyaksha et al., 1989; Ramis et al., 1990).

K_{NH3} in Eq. 11 formally represents the equilibrium constant for adsorption of ammonia on the catalyst. In reality, the NH_3 adsorption capacity of SCR catalysts is strictly related to the number and the strength of their acidic sites. Such catalyst properties depend on a number of factors including temperature, concentration of NH_3 itself, the SO_2 content of the gases, the extent of SO_2 converted to SO_3, and the amount of sulfates used in catalyst preparation and of sulfates formed during aging. Since some of these factors are affected by the operating conditions, K_{NH3} should be actually viewed as a complex parameter, and physico-chemical interpretation of its values must be attempted with caution.

Here, we wish to test the adequacy of the one-dimensional SCR reactor model when the kinetic expression is Eq. 11, which is suitable for simulation of industrial SCR installations.

In the case of the one-dimensional treatment, the dimensionless concentrations of NH_3 in the gas (Γ_{NH3}) and at the catalyst surface ($\Gamma_{P,NH3}$) are easily obtained from the following material balances:

$$\Gamma_{NH3} = \alpha - (1 - \Gamma_{NO}) \qquad (12)$$

$$Sh_{NO}\ (\Gamma_{NO} - \Gamma_{P,NO}) = Sh_{NH3}\ (D_{NH3}/D_{NO})\ (\Gamma_{NH3} - \Gamma_{P,NH3}) \qquad (13)$$

Equations 12 and 13 equate the conversions of NO and NH_3, and their rates of interphase transport, respectively. Both Sh_{NO} and Sh_{NH3} in Eq. 13 are evaluated according to Eq. 10. The two-dimensional description of the SCR monolith reactor now includes two coupled PDEs like Eq. 1 for the spatial distribution of both NO and NH_3 in the gas phase:

$$\varphi \frac{\partial \Gamma_{NO}}{\partial z^*} = \nabla^2 \Gamma_{NO} \qquad (14)$$

$$\varphi \frac{\partial \Gamma_{NH3}}{\partial z^*} = \frac{D_{NH3}}{D_{NO}} \nabla^2 \Gamma_{NH3} \qquad (15)$$

$$z^* = 0\ \ \Gamma_{NO} = 1;\ \ \Gamma_{NH3} = \alpha$$

$$\left.\begin{aligned} -\frac{\partial \Gamma_{NO}}{\partial n^*} &= Da_{NO}\, R^*(\Gamma_{NO}, \Gamma_{NH3}) \\ -\frac{\partial \Gamma_{NH3}}{\partial n^*} &= Da_{NH3}\, R^*(\Gamma_{NO}, \Gamma_{NH3}) \end{aligned}\right\} \text{at the catalytic wall}$$

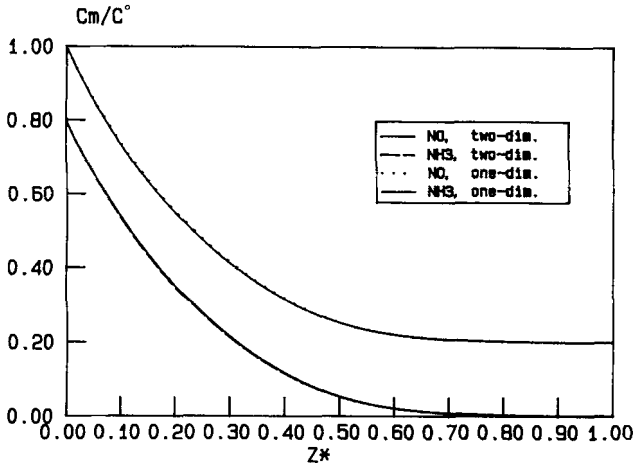

Figure 5. One-dimensional vs. two-dimensional monolith reactor models.

Calculated axial concentration profiles of NO and NH_3; square channels; Rideal kinetics, $Da = 1$, $K^*_{NH3} = 100$.

with dimensionless rate of reaction:

$$R^*(\Gamma_{NO}, \Gamma_{NH3}) = \frac{K^* \Gamma_{NH3}}{1 + K^* \Gamma_{NH3}} \Gamma_{NO} \qquad (16)$$

For representative SCR conditions, axial concentration profiles of NO and NH_3 were calculated by the two-dimensional and the one-dimensional model according to the above equations, and their comparisons were made. Figure 5 indicates that for the square geometry practically no differences are apparent between the two treatments, as in the case of linear kinetics. For the other geometries, at $Da = 1$ the lumped model slightly underpredicted the NO conversion in the circular duct, but slightly overpredicted it in the triangular channel. Again, such deviations appear negligible as far as the conversion of NO is concerned. Nevertheless, they may be of some practical importance when estimating the outlet concentration of ammonia ("NH_3 slip"), which is a critical specification in the design of SCR reactors.

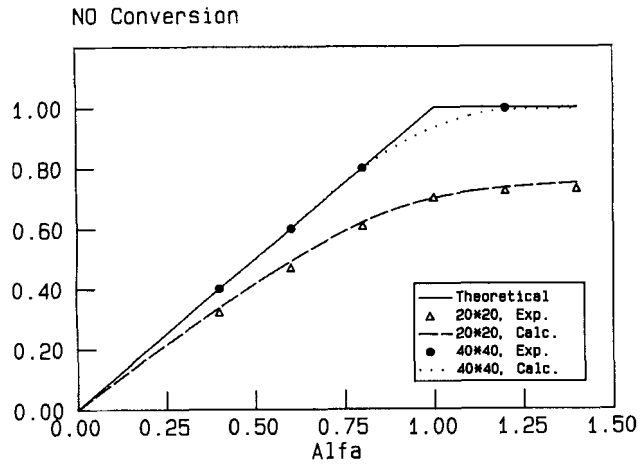

Figure 6. One-Dimensional model for honeycomb catalyst vs. data.

Effect of NH_3/NO feed ratio α on NO conversion. Operating conditions: $T = 380°C$; $AV = 35$ Nm/h (20×20 catalyst); $AV = 12.5$ Nm/h (40×40 catalyst). Kinetic parameters: $Da = 12.1$ D_h (cm), $K^*_{NH3} = 4.71$.

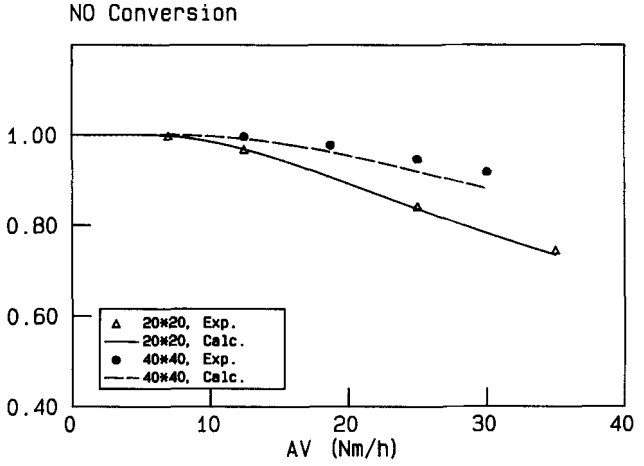

Figure 7. One-Dimensional model for honeycomb catalyst vs. data.

Effect of area velocity AV on NO conversion. Operating conditions: $T = 380°C$, $\alpha = 1.2$. Kinetic parameters as in Figure 6.

In fact, when $\alpha < 1$, the residual concentration of NH_3 is very small near the reactor outlet, so that the absolute differences between the predictions of the two models become significant. For example, calculations show that in the case of a triangular channel geometry ($Da = 1$, $\alpha = 0.8$, $C^\circ_{NO} = 500$ ppm), a reactor simulation based on the one-dimensional model—not a conservative design in this case—would result in underestimating the NH_3 slip by over 2 ppm with respect to a specified upperbound of 5 ppm. On the contrary, a one-dimensional design for the circular geometry would be conservative in this regard, whereas in the case of the square cross-section the lumped model would yield nearly the exact result. Noticeably, a more conservative design for the triangular channel can be achieved by replacing $Nu_{\infty,T}$ with $Nu_{\infty,H}$ in Eq. 10.

In the above calculations, the computer time for solution of the two-dimensional model equations was one (circle) to two (triangle) orders of magnitude greater than required for the lumped model.

The distributed parameter model of the SCR reactor, Eqs.

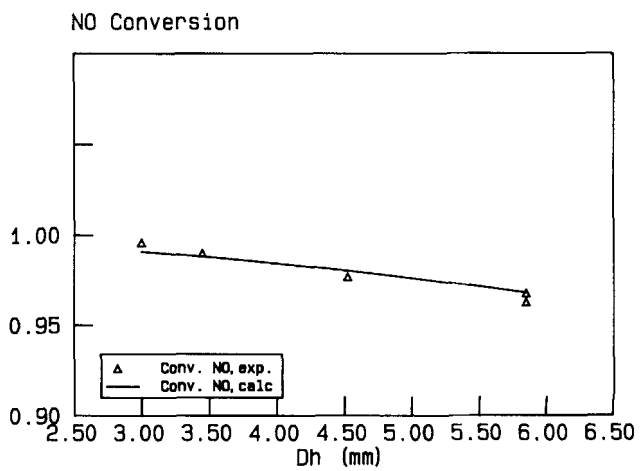

Figure 8. One-Dimensional Model for honeycomb catalyst vs. data.

Effect of channel diameter D_h on NO conversion. Operating conditions: $T = 380°C$, $AV = 12.5$ Nm/h. Kinetic parameters as in Figure 6.

14-16, assumes a fully developed velocity profile. Likewise, the lumped parameter model, Eqs. 9-13, relies on values of Sh based on solutions of thermal entrance problems with a developed velocity profile. The adequacy of this assumption for SCR conditions has been studied by replacing Eq. 10 with Eq. 17 for evaluation of the local Sherwood number in the one-dimensional model:

$$Sh = Nu_{\infty,T} + 8.827\ (1{,}000\ z^*)^{-0.545} \exp\ (-48.2\ z^*) \quad (17)$$

Equation 17 was derived by fitting values of the Nusselt number calculated by Hwang (1974), who numerically solved the combined hydrodynamic and thermal entry problem for $Pr = 0.7$. Thus, Eqs. 9 and 17, which assume implicitly $Sc = 0.7$, provide a lumped model accounting approximately for the development of both the velocity and the concentration profile along the SCR monolith channels. As expected, such a model predicts slightly greater conversions because of the developing momentum boundary layer; however, when compared with the lumped model based on Eq. 10, the departures appear negligible but for very small values of the axial coordinate z^*. Since the effects associated with the development of the velocity profile seem marginal as compared to the experimental uncertainties, they will be neglected in the following.

Comparison with data of honeycomb catalysts

In this section, we compare experimental data of NO conversion in SCR monolith catalysts with corresponding values calculated according to the one-dimensional treatment, Eqs. 9, 10, 12 and 13, with the rate expression in Eq. 11. We intend to demonstrate how the treatment of the SCR reactor discussed in the previous sections represents the behavior of actual SCR systems under different conditions. A thorough analysis of the effects associated with the major operating variables will be addressed in a future article.

The experimental data presented in the following figures are taken from Binder-Begsteiger et al. (1990) and from Binder-Begsteiger (1991). They were obtained in commercial monolith catalysts with square channel diameters approximately in the range 3-6 mm.

Figures 6-8 compare experimental and calculated NO conversions. The two kinetic parameters (k_c and K_{NH3}) for the calculated curves were estimated by global nonlinear regression techniques (Buzzi-Ferraris, 1970) on 22 data points. A single set of parameter values was used in fitting all the data for monoliths of different diameters, since they shared the same chemical composition according to Binder-Begsteiger et al. (1990). The final average percent error of the regression was only 1.3%.

Figure 6, showing the observed and calculated effects of the NH_3/NO feed ratio α on NO conversion for two different situations, confirms that the Rideal rate equation is suitable to represent the reactor behavior over the whole range of α, avoiding any discontinuities between values below and above the stoichiometric ratio ($\alpha = 1$). An agreement between calculation and experiment similar to that in Figure 6 was achieved also with other sets of data measured in our laboratory over different commercial SCR catalysts (Tronconi et al., 1992). In this case, however, the rate parameters had been estimated independently from test runs at very high flow rates, where the influence of interphase mass transport was found negligible. Therefore, the match between computational and experimental results could be achieved here on a predictive basis.

For the same catalysts of Figure 6, Figure 7 shows calculated and experimental effects of the contact time, customarily expressed in the SCR technical literature as area velocity (AV) and defined as:

$$AV = Q/(4\ D_h\ z) = u_m\ D_h/(4\ z) = \frac{D_{NO}}{4\ D_h}\ \frac{1}{z^*} \quad (18)$$

Given the inverse relationship between AV and the dimensionless reactor length z^* (Eq. 18), and the dependence of the Sherwood number on z^* (Eq. 10), it is apparent that a modification of the area velocity affects also the values of the mass transfer coefficients. Therefore, the satisfactory agreement between calculations and experiment in Figure 7 supports the treatment of interphase mass transfer adopted in this work.

Additional support is provided by Figure 8, where calculated and experimental effects of varying the monolith channel diameter are contrasted for the same AV. Note that such effects are entirely due to the influence of interphase diffusional phenomena: as indicated by Figure 8, they can be successfully predicted by the one-dimensional analysis of the SCR reactor.

Finally, Binder-Begsteiger et al. (1990) present also interesting evidence that the NO conversion is unaffected by changing the linear gas velocity in the monolith channels and simultaneously varying the monolith length so that AV remains constant. According to Eq. 18, constant AV (with constant D_h) implies constant z^*. Thus, the SCR model, where NO conversion is a function of only z^*, again predicts the same behavior as observed in practice.

Conclusions

The parametric study of the interaction between kinetics of the chemical reaction at the catalytic wall and gas-solid mass transfer inside isothermal monolith reactors has revealed that mass transfer coefficients estimated from the analogy with the Graetz-Nusselt problem with constant wall temperature may be in error up to about ±20%, depending on the kinetics (Damkohler number) as well as on the channel geometry. Errors to a similar extent are expected if the mass transfer coefficients are determined experimentally in the absence of chemical reaction.

For linear kinetics, however, such errors in the estimates of the mass transfer coefficients do not seriously affect the calculation of NO conversion along the length of the monolith reactor by conventional one-dimensional models, so that their use for this purpose appears adequate. This is still true also for Rideal kinetics with substoichiometric NH_3/NO feed ratios, but calculation of the NH_3 slip is more sensitive: for equilateral triangular monolith channels, representative of a class of plate-type catalysts, mass transfer coefficients based on solutions of the Graetz-Nusselt problem with constant wall temperature result in underestimating the NH_3 outlet concentration. More conservative predictions can be obtained in this case using mass transfer coefficients derived from the Graetz-Nusselt problem with constant wall heat flux.

Notably, a lumped parameter reactor model relying on the analogy with the Graetz-Nusselt problem turns out to be a

very good approximation for the square channel geometry, where mass transfer coefficients are highly insensitive to the influence of the kinetics due to compensation effects. Square channels are most common in honeycomb SCR catalysts.

In addition to comparing satisfactorily with the exact distributed parameter model, the simple one-dimensional treatment of the SCR monolith reactor with honeycomb catalyst is also suitable to reproduce experimental effects of the area velocity and of the channel diameter, which are strictly related to the influence of gas-solid diffusional resistances. When Rideal kinetics are incorporated, the effects of varying the NH_3/NO feed ratio can be effectively reproduced in a continuous fashion. On the other hand, the computation time required for model solution is smaller by one to two orders of magnitude than for the two-dimensional model, depending on the channel geometry. Thus, the lumped parameter model based on Eqs. 9, 10, 12, 13 and 16 appears as a promising tool for the analysis and design of SCR reactors, and can be extended with confidence to include the effects of the catalyst pore structure.

Acknowledgment

This work was performed for ENEL-CRTN (Pisa) under contract No. U026. The authors thank Dr. L. L. Hegedus for providing a copy of his article on design of SCR catalysts before its publication.

Notation

AV = area velocity, Eq. 18, cm/s (or Nm/h)
C = gas-phase concentration, mol/cm^3
c_p = specific heat, cal/(g·K)
Da = $(k_c D_h/D_{NO})$, Damkohler number
D_h = hydraulic diameter of monolith channel, cm
D_{NO} = molecular diffusivity of NO, cm^2/s
D_{NH3} = molecular diffusivity of NH_3, cm^2/s
h = gas-solid heat transfer coefficient, cal/(cm^2·s·K)
k_c = effective rate constant of chemical reaction, cm/s
k_g = gas-solid mass transfer coefficient, cm/s
K_{NH3} = adsorption constant of NH_3, cm^3/mol
K^*_{NH3} = $(K_{NH3} C_{NO}°)$, dimensionless K_{NH3}
k_t = thermal conductivity, cal/(cm·s·K)
n = outward coordinate normal to the monolith wall, cm
Nu = $(h D_h/k_t)$, Nusselt number
Pe = $(u_m D_h/D_{NO})$, Peclet number
Pr = $(c_p \mu/k_t)$, Prandtl number
Q = volumetric gas flow rate, cm^3/s (or Nm^3/h)
r = radial coordinate in channel geometry, cm
R = rate of reaction, mol/(cm^2·s)
R^* = $[R/(k_c C_{NO}°)]$, dimensionless rate of reaction
r^* = r/D_h, dimensionless r-coordinate
Re = $(\rho u D_h/\mu)$, Reynolds number
S = cross-sectional area, cm^2
Sc = $(\mu/\rho D_{NO})$, Schmidt number
Sh_{NO} = $(k_g D_h/D_{NO})$, Sherwood number for NO
u = gas linear velocity, cm/s
x = transverse coordinate in channel geometry, cm
x^* = x/D_h, dimensionless x-coordinate
y = transverse coordinate in channel geometry, cm
y^* = y/D_h, dimensionless y-coordinate
z = axial distance in monolith reactor, cm
z^* = $(z D_{NO}/u_m D_h^2)$, dimensionless z-coordinate

Greek letters and symbols

α = NH_3/NO feed ratio
Γ = $(C/C_{NO}°)$, dimensionless gas-phase concentration
Θ = fractional surface coverage
μ = viscosity, g/(cm·s)
ρ = gas density, g/cm^3
φ = u/u_m, dimensionless velocity profile
∇ = Laplacian operator

Subscripts and superscripts

m = cup-mixing cross-sectional average
P = peripheral average on contour of channel section
T = solution for constant wall temperature
H = solution for constant heat flux
$°$ = at reactor inlet conditions
$*$ = dimensionless quantity
∞ = asymptotic value for $z^* \to \infty$

Literature Cited

Beekman, J. W., and L. L. Hegedus, "Design of Monolith Catalysts for Power Plant NO_x Emission Control," *Ind. Eng. Chem. Res.*, **30**, 969 (1991).

Binder-Begsteiger, I., G. W. Herzog, E. Megla, and M. Tomann-Rosos, "Zur Kinetic der Denox-Reaktion an TiO_2/WO_3-Wabenkatalysatoren," *Chem.-Ing.-Tech.*, **62**(1), 60 (1990).

Binder-Begsteiger, I., personal communication (1991).

Boer, F. P., L. L. Hegedus, T. R. Gouker, and K. P. Zak, "Controlling Power Plant NO_x Emissions," *CHEMTECH*, p. 312, (May, 1990).

Boersma, M. A. M., W. H. M. Tielen, and H. S. Van Der Baan, "Experimental and Theoretical Study of the Simultaneous Development of the Velocity and Concentration Profiles in the Entrance Region of a Monolithic Converter," *ACS Symp. Ser.*, **65**, 72 (1978).

Bosch, H., and F. Janssen, "Catalytic Reduction of Nitrogen Oxides," *Catal. Today*, **2**, 369 (1988).

Brauer, H., and Schlüter, H., "Konvektiver Stoffaustausch mit heterogener chemischer reaktion," *Chem.-Ing.-Tech.*, **37**, 1107 (1965).

Bräuer, H. W., and F. Fetting, "Stofftransport bei Wandreaktion im Einlaufgebiet eines Strömungsrohres," *Chem.-Ing.-Techn.*, **38**, 30 (1966).

Buzanowski, M. A., and R. T. Yang, "Simple Design of Monolith Reactor for Selective Catalytic Reduction of NO for Power Plant Emission Control," *Ind. Eng. Chem. Res.*, **29**, 2074 (1990).

Buzzi-Ferraris, G., "An Optimization Method for Multivariable Functions," Working Party on Routine Computer Programs and the Use of Computers in Chemical Engineering, Florence, Italy (1970).

Carberry, J. J., and A. A., Kulkarni, "The Nonisothermal Effectiveness Factor for Monolith Supported Catalysts," *J. Catal.*, **31**, 41 (1973).

Finlayson, B., *Nonlinear Analysis in Chemical Engineering*, McGraw Hill, New York (1980).

Gill, W. N., and M. S. Suwandi, "Some Aspects of Isothermal Laminar Flow Reactors," *AIChE J.*, **9**, 273 (1963).

Grigull, U., and H. Tratz, "Thermischer Einlauf in ausgebildeter laminarer Rohrströmung," *Int. J. Heat Mass Transfer*, **8**, 669 (1965).

Hawthorn, R. D., "Afterburner Catalysts. Effects of Heat and Mass Transfer between Gas and Catalyst Surface," *AIChE Symp. Ser.*, **137**, 428 (1974).

Heck, R. H., J. Wei, and J. R. Katzer, "Mathematical Modelling of Monolithic Catalysts," *AIChE J.*, **22**, 477 (1976).

Hegedus, L. L., "Temperature Excursions in Catalytic Monoliths," *AIChE J.*, **21**, 849 (1975).

Hlavacek, V., and J. Votruba, "Steady-State Operation of Fixed-Bed Reactors and Monolithic Structures," *Chemical Reactor Theory—A Review*, p. 314, L. Lapidus and N. R. Amundson, eds., Prentice-Hall, Englewood Cliffs, NJ (1976).

Hwang, G. J., and Ja-Pung Sheu, "Effect of Radial Velocity Component on Laminar Forced Convection in Entrance Region of a Circular Tube," *Int. J. Heat Mass Transfer*, **17**, 372 (1974).

Inomata, M., A. Miyamoto, and Y. Murakani, "Mechanism of Reaction of NO and NH_3 on Vanadium Oxide Catalyst in the Presence of Oxygen under the Dilute Gas Condition," *J. Catal.*, **62**, 140 (1980).

Kiovsky, J. R., P. B. Koradia, and C. T. Lin, "Evaluation of a New Zeolitic Catalyst for NO_x Reduction with NH_3," *Ind. Eng. Chem. Prod. Res. Dev.*, **19**, 218 (1980).

Pfefferle, L. D., and W. C. Pfefferle, "Catalysis in Combustion," *Catal. Rev.-Sci. Eng.*, **29**, 219 (1988).

Pereira, C. J., J. E. Kubsh, and L. L. Hegedus, "Computer-Aided Design of Catalithic Monoliths for Automobile Emission Control," *Chem. Eng. Sci.*, **43**, 2087 (1988).

Ramis, G., G. Busca, F. Bregani, and P. Forzatti, "Fourier Transform-Infrared Study of the Adsorption and Coadsorption of Nitric Oxide, Nitrogen Dioxide and Ammonia on Vanadia-Titania and Mechanism of Selective Catalytic Reduction," *Appl. Catal.*, **64**, 259 (1990).

Rajadhyaksha, R. A., G. Hausinger, H. Zeilinger, A. Ramstetter, H. Schmelz, and H. Knözinger, "Vanadia Supported on Titania-Silica. Physical Characterization and Activity for the Selective Reduction on Nitric Oxide," *Appl. Catal.*, **51**, 67 (1989).

Shah, R. K., and A. L. London, *Laminar Flow Forced Convection in Ducts*, Academic Press, New York (1978).

Smith, T. G., and J. J. Carberry, "Design and Optimization of a Tube-Wall Reactor," *Chem. Eng. Sci.*, **30**, 221 (1975).

Taylor, K. C., *Automobile Catalytic Converters*, Springer Verlag, Berlin-New York (1984).

Trimm, D., "Catalytic Combustion (Review)," *Appl. Catal.*, **7**, 249 (1983).

Tronconi, E., and P. Forzatti, J. P. Gomez Martin, and S. Malloggi, "Selective Catalytic Removal of NO_x: a Mathematical Model for Design of Catalyst and Reactor," submitted for publication (1992).

Villadsen, J. V., and M. L. Michelsen, *Solution of Differential Equation Models by Polynomial Approximation*, Prentice-Hall, Englewood Cliffs, NJ (1978).

Villadsen, J. V., and W. E. Stewart, "Solution of Boundary-Value Problems by Orthogonal Collocation," *Chem. Eng. Sci.*, **22**, 1483 (1967).

Votruba, J., O. Mikus, Khue Nguen, V. Hlavacek, and J. Skrivanek, "Heat and Mass Transfer in Honeycomb Catalysts: I," *Chem. Eng. Sci.*, **30**, 117 (1975a).

Votruba, J., O. Mikus, Khue Nguen, V. Hlavacek, and J. Skrivanek, "Heat and Mass Transfer in Honeycomb Catalysts: II," *Chem. Eng. Sci.*, **30**, 201 (1975b).

Wong, W. C., and K. Nobe, "Reduction of NO with NH_3 on Al_2O_3- and TiO_2-Supported Metal Oxide Catalysts," *Ind. Eng. Chem. Prod. Res. Dev.*, **25**, 179 (1986).

Young, L. C., "The Application of Orthogonal Collocation to Laminar Flow Heat and Mass Transfer in Monolith Converters," PhD Thesis, Univ. of Washington, Seattle (1974).

Young, L. C., and B. A. Finlayson, "Mathematical Models of the Monolith Catalytic Converter: I," *AIChE J.*, **22**, 331 (1976a).

Young, L. C., and B. A. Finlayson, "Mathematical Models of the Monolith Catalytic Converter: II," *AIChE J.*, **22**, 343 (1976b).

Manuscript received Apr. 5, 1991, and revision received Nov. 18, 1991.